

See discussions, stats, and author profiles for this publication at: <https://www.researchgate.net/publication/49691223>

# Molecular Dynamics Simulations of the Interfacial and Structural Properties of Dimethyldodecylamine-N-Oxide Micelles

ARTICLE in LANGMUIR · JANUARY 2011

Impact Factor: 4.46 · DOI: 10.1021/la1031416 · Source: PubMed

---

CITATIONS

8

---

READS

20

4 AUTHORS, INCLUDING:



**Chris Lorenz**

King's College London

77 PUBLICATIONS 1,725 CITATIONS

SEE PROFILE



**Chien-Ming Hsieh**

Northeast Institute of Geography and Agro...

8 PUBLICATIONS 17 CITATIONS

SEE PROFILE



**Jayne Lawrence**

King's College London

159 PUBLICATIONS 3,194 CITATIONS

SEE PROFILE

## Molecular Dynamics Simulations of the Interfacial and Structural Properties of Dimethyldodecylamine-N-Oxide Micelles

Christian D. Lorenz,<sup>\*,†</sup> Chien-Ming Hsieh,<sup>‡</sup> Cécile A. Dreiss,<sup>‡</sup> and M. Jayne Lawrence<sup>‡</sup>

<sup>†</sup>Materials and Molecular Modelling Group, Department of Physics, King's College London, London, United Kingdom WC2R 2LS, and <sup>‡</sup>Molecular Biophysics Group, School of Biomedical and Health Sciences, Pharmaceutical Science Division, King's College London, London, United Kingdom SE1 9NH

Received August 7, 2010. Revised Manuscript Received October 10, 2010

A series of large-scale atomistic molecular dynamics simulations were conducted to study the structural and interfacial properties of nonionic dimethyldodecylamine-*N*-oxide (DDAO) micelles with an aggregation number of 104 in pure water, which was determined using small-angle neutron scattering (SANS). From these simulations, the micelles were found to be generally ellipsoidal in shape with axial ratios of  $\sim 1.3$ – $1.4$ , which agrees well with that found from small-angle neutron scattering measurements. The resulting micelles have an area per DDAO molecule of  $94.8 \text{ \AA}^2$  and an average number of hydration water molecules per DDAO molecule of  $\sim 8$ . The effect of the encapsulation of ethyl butyrate ( $\text{CH}_3(\text{CH}_2)_2\text{COOCH}_2\text{CH}_3$ ,  $\text{C}_4$ ) and ethyl caprylate ( $\text{CH}_3(\text{CH}_2)_6\text{COOCH}_2\text{CH}_3$ ,  $\text{C}_8$ ) on the structural and interfacial properties of the nonionic DDAO aggregates was also examined. In the presence of the  $\text{C}_4$  oil molecules, the aggregates were found to be less ellipsoidal and more spherical than the pure DDAO micelles, while the aggregates in the presence of the  $\text{C}_8$  oil molecules were almost perfect spheres. In addition, the  $\text{C}_4$  oil molecules move into the core of the aggregates, while the  $\text{C}_8$  oil molecules stay in the headgroup region of the aggregates. Finally, the structural properties of two micelles formed from different starting states (a “preassembled” sphere and individual DDAO molecules distributing in water) were found to be nearly identical.

### 1. Introduction

Surfactants have been attracting a significant amount of interest for their usefulness in various practical applications including those in the food, cosmetics, and pharmaceutical industries.<sup>1</sup> This wide usage is due to the fact that surfactants display diverse structures in aqueous environments depending on their concentration, the temperature, pH, and the presence of other species in the system (i.e., ions and oils). Specifically, surfactants form aggregates when their concentration in water exceeds the critical micelle concentration. A surfactant consists of both a hydrophobic tail and a hydrophilic headgroup, where the interaction between the surfactant tail and water molecules plays a large role in the nature of the resulting aggregate, i.e., whether the surfactants form micelles or a lamellar phase, for example.

The micelle-forming surfactant, dodecyl dimethylamine oxide (DDAO,  $\text{CH}_3(\text{CH}_2)_{11}\text{N}(\text{CH}_3)_2\text{O}$ ), comprises an amine oxide functional group and has been utilized in many chemical and technological applications. The ionic nature of DDAO depends on the pH of the solution. DDAO molecules are nonionic at  $\text{pH} \geq 7$ , and cationic at  $\text{pH} \leq 3$ , while a nonionic–cationic mixture of DDAO molecules exists for pH between 3 and 7.<sup>2</sup> Therefore, the surface charge density of a DDAO micelle can be varied precisely via pH adjustment, which results in changing the degree of protonation of the amine oxide headgroup.

The structure of the micelles formed from either the nonionic or the cationic form of DDAO, as well as a mixture of each, has been the focus of a significant amount of experimental research covering the past five decades. The first study of DDAO micelles occurred in 1962 when Herrmann used light scattering methods in order to determine the aggregation number of nonionic DDAO

micelles, which was found to be 76 DDAO molecules/micelle in pure water and 78 DDAO molecules/micelle in a 0.2 M NaCl aqueous solution.<sup>3</sup> Herrmann also used light scattering methods and sedimentation experiments to study the general shape of the micelles formed from nonionic and cationic forms of DDAO.<sup>2</sup> Herrmann found that cationic DDAO micelles in 0.2 M NaBr at pH 3 are large (micelle molecular weight (MW) =  $680\,000 \text{ g} \cdot \text{mol}^{-1}$ ) and rod-like in shape (radius of  $22 \text{ \AA}$  and length of  $730 \text{ \AA}$ ) and that the nonionic DDAO micelles are small (MW =  $17\,300 \text{ g} \cdot \text{mol}^{-1}$ ) and “probably” spherical both in water and in 0.2 M sodium halide. Since these two studies, the dependence of size and shape of the DDAO micelles on pH and ionic strength has been studied extensively over the span of the past five decades.<sup>4–26,28</sup>

- (3) Herrmann, K. W. *J. Phys. Chem.* **1962**, *66*, 295.
- (4) Benjamin, L. J. *J. Phys. Chem.* **1964**, *68*, 3575.
- (5) Tokiwa, F.; Ohki, K. *J. Phys. Chem.* **1966**, *70*, 3437.
- (6) Goddard, E. D.; Kung, H. C. *J. Colloid Interface Sci.* **1973**, *43*, 511.
- (7) Maeda, H.; Tsunoda, M.; Ikeda, S. *J. Phys. Chem.* **1974**, *78*, 1086.
- (8) Funasaki, N. *J. Colloid Interface Sci.* **1977**, *60*, 54.
- (9) Ikeda, S.; Tsunoda, M.; Maeda, H. *J. Colloid Interface Sci.* **1978**, *67*, 336.
- (10) Ikeda, S.; Tsunoda, M.; Maeda, H. *J. Colloid Interface Sci.* **1979**, *70*, 448.
- (11) Mille, M. *J. Colloid Interface Sci.* **1981**, *81*, 169.
- (12) Chang, D. L.; Rosano, H. L.; Woodward, A. E. *Langmuir* **1985**, *1*, 669.
- (13) Warr, G. G.; Grieser, F.; Evans, D. F. *J. Chem. Soc., Faraday Trans. 1* **1986**, *82*, 1829.
- (14) Maeda, H. *J. Phys. Chem.* **1988**, *92*, 4490.
- (15) Abe, A.; Imae, T.; Shibuya, A.; Ikeda, S. *J. Surf. Sci. Technol.* **1988**, *4*, 67.
- (16) Rathman, J. F.; Christian, S. D. *Langmuir* **1990**, *6*, 391.
- (17) Uchiyama, H.; Christian, S. D.; Scameborn, J. F.; Abe, M.; Ogino, K. *Langmuir* **1991**, *7*, 95.
- (18) Zhang, H.; Dubin, P. L.; Kaplan, J. I. *Langmuir* **1991**, *7*, 2103.
- (19) Brackman, J. C.; Engberts, J. B. F. N. *Langmuir* **1992**, *8*, 424.
- (20) Imae, T.; Hayashi, N. *Langmuir* **1993**, *9*, 3385.
- (21) Kaimoto, H.; Shoho, K.; Sasaki, S.; Maeda, H. *J. Phys. Chem.* **1994**, *98*, 10243.
- (22) Maeda, H.; Muroi, S.; Ishii, M.; Kakehashi, R.; Kaimoto, H.; Nakahara, T.; Motomura, K. *J. Colloid Interface Sci.* **1995**, *175*, 497.
- (23) Maeda, H. *Colloids Surf., A: Physicochem. Eng. Aspects* **1996**, *109*, 263.
- (24) Maeda, H.; Muroi, S.; Kakehashi, R. *J. Phys. Chem. B* **1997**, *101*, 7378.
- (25) Terada, Y.; Maeda, H.; Odagaki, T. *J. Phys. Chem. B* **1997**, *101*, 5784.

\*To whom correspondence should be addressed. E-mail: chris.lorenz@kcl.ac.uk.

(1) Thadros, Th. F. *Applied Surfactants*; Wiley-VCH, 2005.  
(2) Herrmann, K. W. *J. Phys. Chem.* **1964**, *68*, 1540.

In this paper, the shape and the structural and interfacial properties of nonionic DDAO micelles in pure water are the focus. Since the first paper by Herrmann in 1962,<sup>3</sup> several other experimental studies have been conducted investigating the size and shape of pure nonionic DDAO micelles. Chang et al.<sup>12</sup> found from carbon-13 NMR results that the micelles formed from nonionic DDAO molecules are spherical in shape. Orädd et al.<sup>29</sup> observed that the aggregation number of pure nonionic DDAO micelles increased from 75 to 95 as the concentration of DDAO increased from 2% to 20% w/w using a time-resolved fluorescence (TRF) quenching technique. Also, their pulsed field gradient FT-NMR studies showed a broad distribution of micelle sizes, including at low concentrations of DDAO (<6% w/w) where the micelles seemed to be spherical with a radius of 19.6 Å but they did not expect the micelles to remain spherical at higher concentrations of DDAO. Maeda et al.<sup>24</sup> measured a radius of ~20 Å for the equivalent hydrodynamic sphere of nonionic DDAO micelles using dynamic light scattering and stated that the micelles were thought to be spherical in shape. Garamus et al.<sup>26</sup> used small-angle neutron scattering (SANS) measurements and found an aggregation number of  $78 \pm 2$  for the nonionic DDAO micelles, which were ellipsoidal in shape with semi axis of rotation of  $(46 \pm 3, 30 \pm 2)$ . Most recently, Barlow et al.<sup>30</sup> reported experimental results from SANS measurements, in which they determined that the nonionic DDAO micelles have an aggregation number of 104 and established that the micelles were prolate ellipsoids with an axial ratio of 1.6–1.7.

In the following sections, the results from a series of atomistic molecular dynamics simulations of nonionic DDAO micelles in water and in the presence of short (ethyl butyrate,  $\text{CH}_3(\text{CH}_2)_2\text{COOCH}_2\text{CH}_3$ ) and medium chain length (ethyl caprylate,  $\text{CH}_3(\text{CH}_2)_6\text{COOCH}_2\text{CH}_3$ ) ethyl ester oil molecules are reported. Previously, Sterpone et al.<sup>27</sup> have studied the dynamical properties of interfacial water molecules near DDAO micelles, but they did not study the properties of the micelle or of the aggregation of the surfactant molecules to form the micelle. Therefore, to the authors' knowledge, the work presented in this manuscript represents the first such study of the properties of the micelle and the effects of ethyl ester oil molecules on the physical properties of microemulsions containing DDAO.

In this study, the aggregation number reported by Barlow et al.<sup>30</sup> has been used as a starting point. In doing so, two different initial structures were used: (1) the DDAO molecules are placed in a “preassembled” spherical micelle and (2) the DDAO molecules are placed on equally spaced vertices of a cubic grid, surrounded by water molecules and then allowed to self-assemble into a micelle. In both cases, the resulting micelle is nearly identical in shape and size, and the micelle is found to be ellipsoidal in shape with an axial ratio of ~1.3–1.4 and has an area per DDAO molecule as measured at the outer surface of  $94.8 \text{ Å}^2$ , which agrees well with the experimental values obtained from SANS measurements by Barlow et al.<sup>30</sup> The structure of the micelle in the presence of the short and medium chain ethyl ester oil molecules (known also as a microemulsion) was also investigated. The results show that the aggregate in the presence of either oil is larger than in its absence, and that the aggregate containing the  $\text{C}_4$

oil molecules is larger than that containing the  $\text{C}_8$  oil molecules. Also, the shape of the aggregate was found to be more spherical in the presence of either oil than when there is no oil present, and the aggregate in the presence of  $\text{C}_8$  oil molecules is nearly a perfect sphere, while the aggregate formed in the presence of the  $\text{C}_4$  oil is still slightly ellipsoidal. The short chain  $\text{C}_4$  oil molecules were found to be more prevalent in the core of the aggregates than the medium chain  $\text{C}_8$  oil molecules, which is opposite to the experimentally observed trend by Barlow et al., when they studied the location of  $\text{C}_8$  and  $\text{C}_{16}$  oil molecules in the microemulsions formed with DDAO molecules.<sup>30</sup> In addition to the structure of the DDAO micelles, the interfacial properties of the micelles with water molecules and the hydration numbers and the hydrogen bonding properties of the DDAO micelles were measured.

The next section of this paper introduces the specifics of the various simulations conducted. The results of the simulations from the “preassembled” nonionic DDAO molecule in pure water are presented in section 3.1. The effect of adding the  $\text{C}_4$  and  $\text{C}_8$  ethyl ester oil molecules on the structural and interfacial properties of the aggregates is presented in section 3.2. The structure of the self-assembled micelle is compared to the structure resulting from the equilibration of the “preassembled” micelle in section 3.3. Finally, the major findings of this study are summarized in section 4.

## 2. Description of Simulations

A series of all-atom molecular dynamics (MD) simulations were conducted in order to understand the interfacial and structural properties of micelles consisting of the zwitterionic surfactant DDAO in water. In all simulations, 104 DDAO molecules, as obtained experimentally from SANS measurements,<sup>30</sup> were used, and the structural and interfacial properties of the DDAO micelle that resulted from two different starting configurations were studied. In one system, the locations of 104 equally spaced grid points on the surface of a sphere with diameter of 19.4 Å were initially determined. Then, DDAO molecules were built such that the methyl group at the end of the hydrocarbon chains were placed at each vertex (see Figure 1a). Similar methods have been used in several previous simulation studies of various types of micelles.<sup>31–33</sup> Then, an energy minimization and a brief (~1 ps) thermalization simulation of only the micelle were conducted at  $T = 300 \text{ K}$ , before placing the resulting structure into a  $100 \text{ Å} \times 100 \text{ Å} \times 100 \text{ Å}$  box of water (see Figure 1b). Finally, another energy minimization was performed with the micelle in the water box, and the system was thermalized first in NPT conditions for 100 ps and then in NVT conditions for 100 ps. The production simulation was then conducted at 300 K under NVT conditions. This production simulation lasted 10 ns, and all of the measurements discussed in the following sections were conducted in the last 5 ns.

In the other system, the DDAO molecules were initially placed on equally spaced vertices of a cubic grid within a simulation box with dimensions of  $100 \text{ Å} \times 100 \text{ Å} \times 100 \text{ Å}$ . The DDAO molecules were initially placed such that their center of mass was roughly 10 Å removed from neighboring DDAO molecules in the  $x$  and  $y$  dimensions, and they were all oriented in the same way such that their long axis was in the  $z$  dimension and the tail of each molecule was approximately 8 Å removed from the head of the nearest-neighbor molecule in the  $z$  dimension. Then, water

(26) Garamus, V.; Kameyama, K.; Kakehashi, R.; Maeda, H. *Colloid Polym. Sci.* **1999**, *277*, 868.

(27) Sterpone, F.; Marchetti, G.; Pierleoni, C.; Marchi, M. *J. Phys. Chem. B* **2006**, *110*, 11504.

(28) Maeda, H.; Kakehashi, R. *Adv. Colloid Interface Sci.* **2000**, *88*, 275.

(29) Orädd, G.; Lindblom, G.; Johansson, L. B. Å.; Wikander, G. *J. Phys. Chem.* **1992**, *96*, 5170.

(30) Barlow, D. J.; Lawrence, M. J.; Zuberi, S.; Heenan, R. K. *Langmuir* **2000**, *16*, 10398.

(31) MacKerell, A. D. *J. Phys. Chem.* **1995**, *99*, 1846.

(32) Bruce, C. D.; Senapati, S.; Berkowitz, M. L.; Perera, L.; Forbes, M. D. E. *J. Phys. Chem. B* **2002**, *106*, 10902.

(33) Shang, B. Z.; Wang, Z.; Larson, R. G. *J. Phys. Chem. B* **2008**, *112*, 2888.



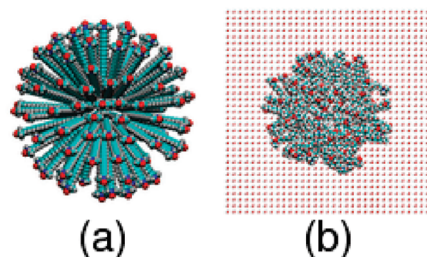


**Figure 1.** Snapshots of (a) the initial configuration where the 104 DDAO molecules are placed on equally spaced grid points on the surface of a sphere, and (b) after an energy minimization and a short ( $\sim 1$  ps) thermalization the micelle is placed into a  $100 \text{ \AA} \times 100 \text{ \AA} \times 100 \text{ \AA}$  box of water. The different colors represent the different elements in the system: oxygen - red, nitrogen - blue, carbon - cyan, hydrogen - white.

was placed into the box such that the number of water molecules placed in the system resulted in an equilibrium density of water of  $1 \text{ g/cm}^3$ . Next, a series of minimization and NPT ( $\sim 100$  ps) and NVT ( $\sim 100$  ps) simulations were conducted in order to thermalize the system at 300 K. The temperature of the system was then raised to 400 K in order to speed up the diffusion dynamics of the surfactant chains and then a NVT simulation was run for 61 ns, at which point the surfactant molecules had self-assembled into a micelle. The temperature was then decreased to 300 K and the system was allowed to equilibrate for approximately 13 ns at this temperature. Over this period of time, the trajectories of the system were collected so that the necessary analysis could be conducted.

The effect of the presence of short ( $\text{C}_4$ ,  $\text{CH}_3(\text{CH}_2)_2\text{COOCH}_2\text{CH}_3$ ) and medium ( $\text{C}_8$ ,  $\text{CH}_3(\text{CH}_2)_6\text{COOCH}_2\text{CH}_3$ ) chain ethyl ester oil molecules on the structural and interfacial properties of the DDAO aggregate was also studied. Here, two separate simulations were conducted to study the effect of the oil molecules on the behavior of the aggregate: one with 104 DDAO molecules and 205  $\text{C}_4$  oil molecules and another with 104 DDAO molecules and 92  $\text{C}_8$  oil molecules. These mixtures of ethyl ester and DDAO molecules were selected on the basis that at these concentrations the ethyl ester oil molecules were close to the maximum amount that could be incorporated into the resulting microemulsions without resulting in phase separation.<sup>34</sup> Each simulation started from a configuration where the oil molecules were placed on randomly picked grid points on the surface of a sphere larger than the micelle and built in a similar way as the surfactant molecules (see Figure 2). The minimum distance between any atom on a surfactant molecule and any atom on an oil molecule in this arrangement is approximately  $7 \text{ \AA}$ , and in all cases, the oil molecules are oriented such that the carboxyl end of the oil is furthest away from the surfactant molecule. Again, an energy minimization and a short ( $\sim 1$  ps) thermalization simulation of only the surfactant and oil molecules were conducted at  $T = 300 \text{ K}$ , before placing them into a  $100 \text{ \AA} \times 100 \text{ \AA} \times 100 \text{ \AA}$  box of water (see Figure 2). As in the system with only DDAO, a series of energy minimization, NPT, and NVT simulations were then conducted in order to thermalize the system in the box of water. Finally, the production simulation was conducted for 10 ns and the data used for the analysis discussed in the following sections was collected over the last 5 ns.

All of the NVT and NPT simulations are conducted using a Nose-Hoover thermostat<sup>35</sup> to control the temperature, and the

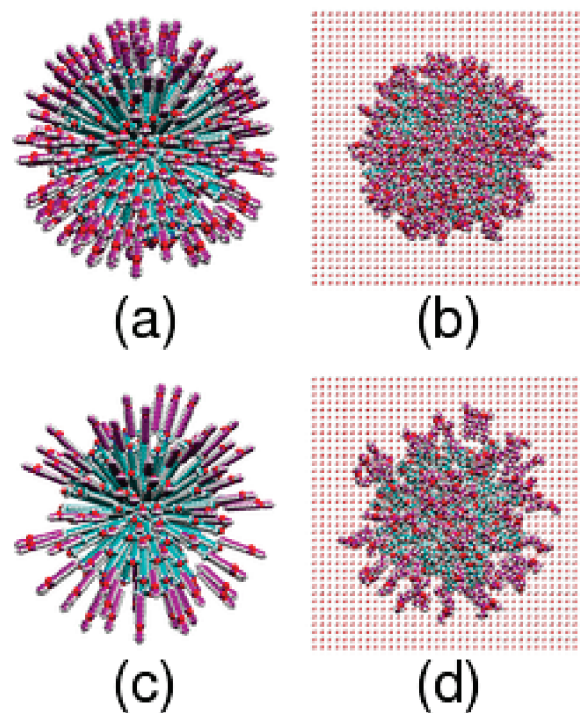


**Figure 2.** Snapshots of  $\text{C}_4$  ethyl ester oil/DDAO and  $\text{C}_8$  ethyl ester oil/DDAO microemulsions. (a) Initial configuration with 104 DDAO molecules placed on equally spaced grid points on the surface of an inner sphere and 205  $\text{C}_4$  oil molecules placed on randomly chosen grid points on the surface of an outer sphere and (b) after an energy minimization and a short ( $\sim 1$  ps) thermalization when the micelle and oil molecules are placed into a  $100 \text{ \AA} \times 100 \text{ \AA} \times 100 \text{ \AA}$  box of water. (c) Initial configuration with 104 DDAO molecules placed on equally spaced grid points on the surface of an inner sphere and 92  $\text{C}_8$  oil molecules placed on randomly chosen grid points on the surface of an outer sphere and (d) after an energy minimization and a short ( $\sim 1$  ps) thermalization when the micelle and oil molecules are placed into a  $100 \text{ \AA} \times 100 \text{ \AA} \times 100 \text{ \AA}$  box of water. The same color scheme is used here as in Figure 1, except that the carbons of the ethyl ester oil molecules are purple in order to differentiate them from the DDAO molecules.

NPT simulations also use a Nose-Hoover barostat<sup>36</sup> that has been implemented as described by Melchionna et al.<sup>37</sup> In each instance, a time step of 2 fs with the velocity Verlet integrator is used, and all hydrogen-containing bonds are constrained using the SHAKE algorithm.<sup>38</sup> All the simulations were performed with the LAMMPS simulation package<sup>39</sup> utilizing the OPLS-AA forcefield<sup>40,41</sup> to describe the inter- and intra-molecular interactions for the colloidal and ether oil molecules, while the TIP3P model was used to describe the interactions of water molecules.<sup>42</sup> The van der Waals interactions and short-range Coulomb interactions were cut off at 1.0 nm, and the PPPM algorithm<sup>43</sup> was used to compute the long-range Coulomb interactions.

(37) Melchionna, S.; Cicotti, G.; Holian, B. L. *Mol. Phys.* **1993**, *78*, 533.

(38) Ryckaert, J. P.; Cicotti, C.; Berendsen, H. J. C. *J. Comput. Phys.* **1977**, *23*, 327.

(39) Plimpton, S. *J. Comp. Phys.* **1995**, *117*, 1, 1995.

(40) Jorgensen, W. J.; Maxwell, D. S.; Tirado-Rives, J. *J. Am. Chem. Soc.* **1996**, *118*, 11225. Jorgensen, W. J. private communication, **2003**.

(41) Jorgensen, W. L.; Chandrasekhar, J.; Madura, L. T.; Impey, R. W.; Klein, M. L. *J. Chem. Phys.* **1983**, *79*, 926.

(42) Jorgensen, W. L.; Chandrasekhar, J.; Madura, L. T.; Impey, R. W.; Klein, M. L. *J. Chem. Phys.* **1983**, *79*, 926.

(43) Hockney, R. W.; Eastwood, J. W. *Computer Simulation Using Particles*; Taylor & Francis: New York, 1989.

(34) Warisnoicharoen, W.; Lansely, A. B.; Lawrence, M. J. *Int. J. Pharm.* **2000**, *198*, 7.

(35) Hoover, W. G. *Phys. Rev. A* **1985**, *31*, 1695.

(36) Hoover, W. G. *Phys. Rev. A* **1985**, *34*, 2499.

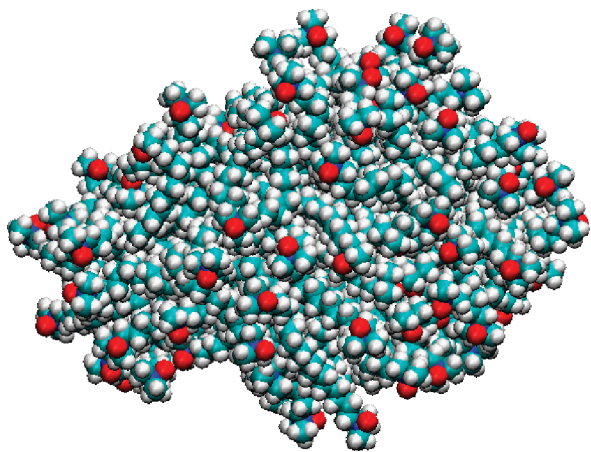


**Figure 3.** Snapshot of the equilibrated DDAO micelle after 10 ns of simulation. The same color scheme is used here as in Figure 1.

### 3. Results

In this section, the results of the pure DDAO micelle as started from the spherical configuration are presented. Next, the results of the simulations of the microemulsions containing DDAO and the  $C_4$  and  $C_8$  ethyl ester oil molecules are shown, and the effect of the oils on the structural and interfacial properties of the aggregates is discussed. Finally, the results of the micelles formed from the two different starting states are compared, and the self-assembly properties of the DDAO micelle are discussed.

**3.1. Preassembled Pure DDAO Micelle.** In order to characterize the general size of the DDAO micelle resulting from the preassembled starting configuration, the root-mean-square (rms) distance of the oxygen atoms in the DDAO molecules and the center of mass of the micelle were determined, and found to result in a micellar radius  $R_s$  of 22.7 Å. In addition, the radius of the hydrocarbon core was found to be 21.5 Å, as determined from the rms distance of the first carbon in the backbone of the DDAO that is connected to the nitrogen and the center of mass of the micelle.

In order to determine the sphericity of the micelle, the moments of inertia along the three principle axes of the micelle ( $I_1$ ,  $I_2$ , and  $I_3$ ) were calculated. The ratios of these principle axes  $I_1/I_3$ ,  $I_2/I_3$ , and  $I_1/I_2$  are 1.52, 1.40, and 1.07, respectively, which show that the micelle is significantly elliptical in shape. Figure 3 shows a snapshot of the equilibrated micelle.

The surface area of the micelle was calculated using a modified version of the rolling ball algorithm<sup>44,45</sup> that was initially developed by Richards.<sup>46</sup> The surface area of the micelle was determined by using a probe of radius 10 Å to allow the calculation of the surface area of only the hull of the micelle, similar to previous work on ribosomes and other biological macromolecules.<sup>44,45</sup> From the result of the surface area calculation, the area per DDAO molecule was determined to be 94.8 Å<sup>2</sup>.

The structure of the micelle is further described by the location of the various atomic species of the DDAO molecules within the micelle. Figure 4a shows the number density of the atomic species as a function of the distance from the center of mass of the micelle. The plot shows, as expected, that the more hydrophilic species of the molecules (nitrogen and oxygen atoms) are near the water interface, while the center of the micelle contains only the hydrocarbon tails of the DDAO molecules.

The interfacial properties of the micelle with the surrounding water are of obvious interest. One measure of its interactions with the surrounding water molecules is the hydrogen bonds that are formed with the micelle and how the micelle itself disturbs the hydrogen bond network of the water around it. A hydrogen bond is determined to exist between a water molecule and another water molecule or a DDAO molecule when an oxygen in a water molecule and an oxygen in either another water molecule or a DDAO molecule that are within 3.5 Å of one another and are positioned such that the  $\text{OH} \cdots \text{O}$  angle of  $> 150^\circ$ <sup>47</sup> was used. In bulk water, the average number of hydrogen bonds per water molecule is 3.3, which is consistent with other simulation studies of hydrogen bonding within bulk water.<sup>48</sup> Nearer the micelle interface, the number of hydrogen bonds per water decreases to 3.0 as the interfacial effect is felt and a disruption of the hydrogen bond network occurs (not shown). Figure 5 shows the fraction of water molecules that have  $n$  (ranging from 1 to 5) hydrogen bonds with other water molecules as well as with the oxygens in the DDAO molecules as a function of the distance from the surface of the micelle. At the micelle interface ( $r < 3.5$  Å), some water molecules form hydrogen bonds with the oxygen atoms in the DDAO molecules. As a result of this hydrogen bonding with the micelle, the number of water molecules with 4 and 5 hydrogen bonds with other water molecules decreases and the number of water molecules with 0–3 hydrogen bonds with other water molecules increases.

Another interfacial property of the water–micelle interface that was measured is the number of hydration water molecules. To do this, the radial distribution functions (r.d.f.) between each atom type in the DDAO micelle and the oxygen in a water molecule were determined. Then, the number of water molecules that are within the distance that corresponds to the first peak in the rdf curve from any atom of a DDAO molecule was counted. In doing so, care was taken not to double count any water molecules that had been previously counted as hydrating another atom of a DDAO molecule. Figure 6 shows a histogram of the number of hydration water molecules for the DDAO molecules. The average value is  $\sim 8$  hydration water molecules per DDAO molecule; however, the distribution is quite broad. Similar numbers of hydration water molecules per DDAO molecule have been found from the analysis of experimental SANS data by Barlow et al.,<sup>30</sup> namely, 4–8 water molecules, while Kakitani et al. used a range of 5.7–8.7 to analyze their SANS data,<sup>49</sup> and from viscosity measurements, hydration levels of 10 water molecules per DDAO molecule were found.<sup>50</sup>

**3.2. Effect of Ethyl Ester Oils on the DDAO Micelles.** As stated previously, the properties of the microemulsions formed in the presence of short ( $C_4$ ) and medium ( $C_8$ ) chain ethyl ester oil molecules were also investigated. First, the radius of the microemulsions,  $R_s$ , and the radius of the hydrocarbon core of each microemulsion were measured (the calculations were conducted in the same manner as described in the previous section) in order to give a measure of the size of the microemulsions in the presence of oil molecules. Also, in order to characterize the general shape of each microemulsion, the moments of inertia along the three primary axes of the microemulsion ( $I_1$ ,  $I_2$ , and  $I_3$ ) were determined and used to calculate the ratio of the various moments:  $I_1/I_3$ ,  $I_2/I_3$ , and  $I_1/I_2$ . Finally, the surface area of the equilibrated microemulsion of each system was determined. Table 1 shows a comparison of these values for the microemulsions that contain the  $C_4$  and the

(44) Voss, N. R.; Gerstein, M.; Steitz, T. A.; Moore, P. B. *J. Mol. Biol.* **2006**, *360*, 893.

(45) Voss, N. R. *Geometric Studies of RNA and Ribosomes, and Ribosome Crystallization*; PhD Dissertation; Yale University, 2007.

(46) Richards, F. M. *Annu. Rev. Biophys. Bioeng.* **1977**, *6*, 151.

(47) Luzar, A.; Chandler, D. *Phys. Rev. Lett.* **1996**, *76*, 928.

(48) Faraudo, J.; Travesset, A. *Biophys. J.* **2007**, *92*, 2806.

(49) Kakitani, M.; Imae, T.; Furusaka, M. *J. Phys. Chem.* **1995**, *99*, 16018.

(50) Courchene, W. I. *J. Phys. Chem.* **1964**, *68*, 1870.

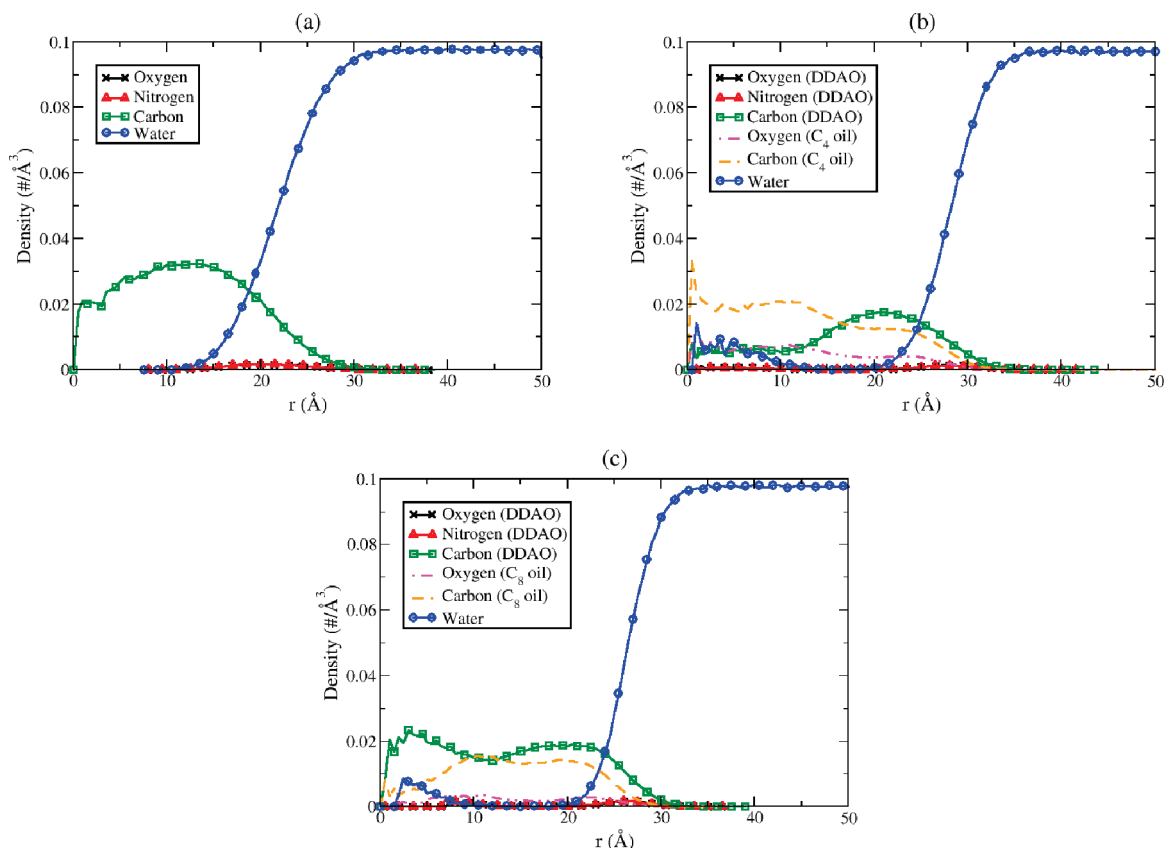


**Figure 4.** Number density of the various atomic species in (a) the pure DDAO micelle in water, (b) the microemulsion of DDAO and C<sub>4</sub> ethyl ester oil molecules in water, and (c) the microemulsion of DDAO and C<sub>8</sub> ethyl ester oil molecules in water. Different colors are used for the different atomic species in the DDAO molecules (oxygen, black ×; nitrogen, red △; carbon, green □), the ethyl ester oil molecules (carbon, orange dashed line; oxygen, pink dash–double dotted line) and the water molecules (blue ○). (Note: The data for the oxygen and the nitrogen atoms of the DDAO molecules lie nearly directly on top of one another, which may make it hard to see the oxygen data in the plot.)

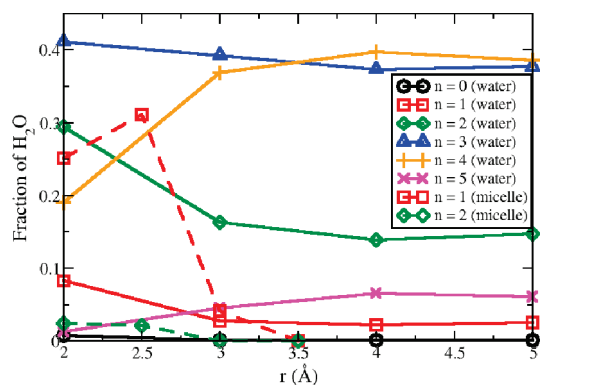


**Figure 5.** Fraction of water molecules that have 0 (black ○), 1 (red □), 2 (green ◇), 3 (blue △), 4 (orange +), and 5 (pink ×) hydrogen bonds with other water molecules (solid lines) and the DDAO molecules (dashed lines).

C<sub>8</sub> ethyl ester oil molecules to those found for the pure DDAO micelles.

In terms of the radius of the aggregates, the aggregates rank in size from largest to smallest: DDAO/C<sub>4</sub> ethyl ester oil molecules > DDAO/C<sub>8</sub> ethyl ester oil molecules > pure DDAO. The same ranking order is observed for the area per DDAO molecule of the aggregates. However, in terms of sphericity, the aggregates rank from most spherical to least spherical: DDAO/C<sub>8</sub> ethyl ester oil molecules > DDAO/C<sub>4</sub> ethyl ester oil molecules > pure DDAO. For visual comparison, snapshots of the equilibrated microemulsions of the DDAO/C<sub>4</sub> ethyl ester oil and DDAO/C<sub>8</sub> ethyl ester

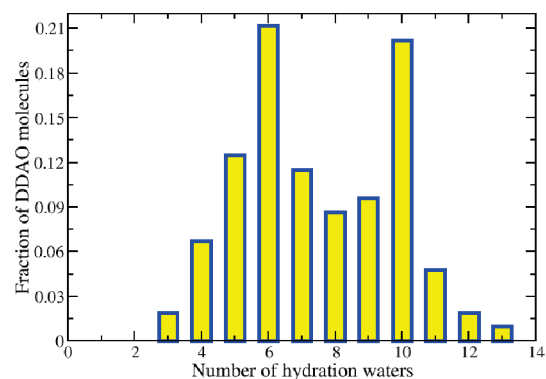


**Figure 6.** Fraction of DDAO molecules that have  $n$  hydration water molecules.

oil systems are given in Figure 7 and the pure DDAO micelle is shown in Figure 3.

In order to determine the structure of the microemulsions, the density of the various atomic species of the DDAO and ethyl ester oil molecules was calculated as a function of distance from the microemulsion's center of mass. Figure 4b,c shows plots of the number density of the various species for the DDAO/C<sub>4</sub> ethyl ester oil and DDAO/C<sub>8</sub> ethyl ester oil systems, respectively. In the case of the DDAO/C<sub>4</sub> ethyl ester oil microemulsion, the oil molecules penetrate the microemulsion and position themselves in the core of the microemulsion for the most part. In doing so, the hydrocarbon chains of the DDAO molecules are displaced from the core of the microemulsion and thus move further from the



center of mass of the microemulsion, nearer the microemulsion/water interface. Also, a few water molecules ( $\sim 3$ ) are taken into the core of the microemulsion with the oil molecules as they diffuse into the microemulsion.

In the case of the DDAO/ $C_8$  ethyl ester oil microemulsion, the oil molecules do not penetrate as deeply into the core of the microemulsion; instead, they populate the region between the hydrophilic head groups of the DDAO and the core of the microemulsion. However, in this case, the oil molecules do not significantly displace any part of the DDAO molecules. As in the DDAO/ $C_4$  ethyl ester oil microemulsions, a few water molecules find their way into the core of the microemulsion along with the oil molecules.

In order to understand the effect that the presence of the two types of oil molecules has on the water/microemulsion interface, the hydrogen bonding behavior of the water with other water molecules and with the DDAO and oil molecules was measured. The hydrogen bonds are measured in the same way as in the previous section. In the systems with  $C_4$  and  $C_8$  ethyl ester oil

molecules, the average number of hydrogen bonds per water molecule decreases from the bulk value to  $\sim 3$  nearer the microemulsion surface, which is the same trend observed in the structure of water near the pure DDAO micelle (not shown).

The number of hydrogen bonds per DDAO and per ethyl ester oil for the different systems were measured. Figure 8a,b shows histograms of the number of hydrogen bonds per DDAO molecules and ethyl ester oil molecules, respectively. Figure 8a shows that the hydrogen bonding between water molecules and DDAO molecules is more or less unperturbed by the presence of the  $C_4$  ethyl ester oil molecules when compared to the pure DDAO system. In both the pure DDAO micelle and the DDAO/ $C_4$  ethyl ester oil microemulsion, the DDAO molecules are hydrogen-bonded to 2.1 water molecules on average. However, in the system with  $C_8$  ethyl ester oil molecules, there is a reduction in the number of hydrogen bonds that are formed between DDAO molecules and water molecules resulting in a drop in the average number of water molecules hydrogen-bonded to a DDAO molecule to 1.9. These results are consistent with what is observed from the structure of the microemulsions, in that the  $C_4$  oil molecules are mostly located within the core of the microemulsion and therefore would not really effect the interfacial behavior. Whereas the  $C_8$  oil molecules are located nearer the interface and can therefore compete with the DDAO molecules for hydrogen bonding with water molecules.

The effect of the presence of the ethyl ester oil molecules on the number of hydration water molecules surrounding the microemulsion was also investigated. The modeling of the experimental SANS data is not very sensitive to the hydration level of the microemulsion droplets due to their large relative size,<sup>30</sup> so in this instance, the results from the simulations can provide further information that is not obtainable from the analysis of SANS data. Using the same methodology described in the previous section, the number of hydration water molecules per DDAO molecule and per ethyl ester oil molecule were calculated for the three different systems and the resulting histograms are shown in Figure 9 (number of hydration water molecules/DDAO molecule) and Figure 10 (number of hydration water molecules/ethyl ester oil molecules). Figure 10 shows that  $C_8$  ethyl ester oil molecules have a larger number of hydration water molecules compared to the  $C_4$  ethyl ester oil molecules. On average, the  $C_8$  ethyl ester oil molecules have 1.8 hydration water molecules, while the  $C_4$  ethyl ester oil molecules have 1.2. Again, these findings are consistent with the structure of the microemulsions that was observed, with the  $C_8$  oil molecules being mostly located nearer the microemulsion/water interface than the  $C_4$  oil molecules.

**Table 1. Comparison of Physical Properties of the Pure DDAO Micelles, and the Microemulsions Formed in the DDAO/ $C_4$  Ethyl Ester Oil and the DDAO/ $C_8$  Ethyl Ester Oil Systems<sup>a</sup>**

property	units	DDAO	DDAO/ $C_4$	DDAO/ $C_8$
$R_s$	Å	22.7	28.2	25.6
$R_h$	Å	21.5	27.0	24.4
$I_1/I_3$		1.52	1.21	1.01
$I_2/I_3$		1.40	1.20	1.01
$I_1/I_2$		1.07	1.01	1.00
Area/DDAO	Å <sup>2</sup>	94.8	138.4	119.6

<sup>a</sup> The properties listed in this table include the aggregate radius  $R_s$ , the hydrocarbon core radius  $R_h$ , the three ratios of the moments of inertia ( $I_1/I_3$ ,  $I_2/I_3$ ,  $I_1/I_2$ ), and the area per DDAO molecule of the aggregate.

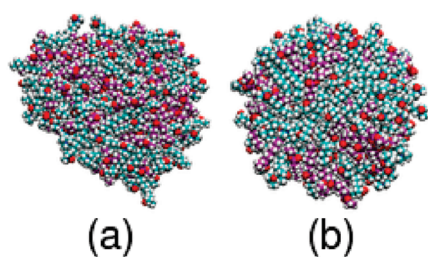


**Figure 7.** Snapshots of the equilibrated (a) DDAO/ $C_4$  ethyl ester oil microemulsion and (b) DDAO/ $C_8$  ethyl ester oil microemulsion after 10 ns of simulation. The same color scheme is used here as in Figure 2.

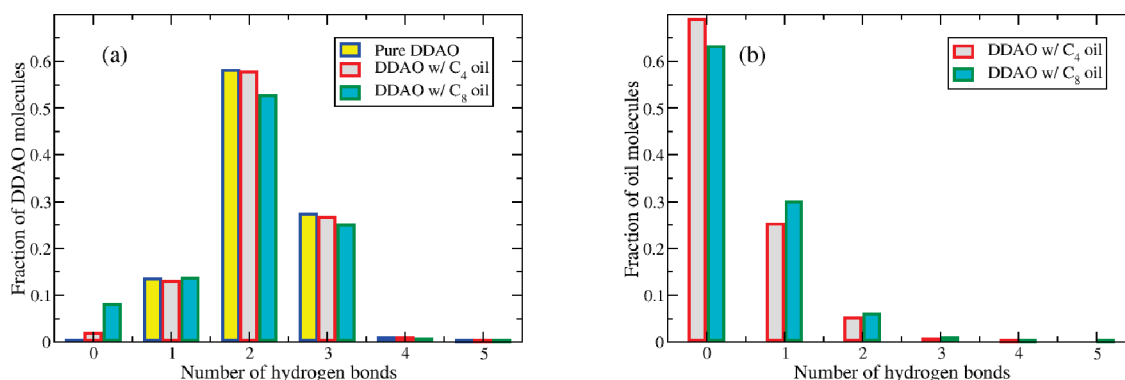


**Figure 8.** (a) Number of hydrogen-bonded water molecules per DDAO molecule. (b) Number of hydrogen-bonded water molecules per ethyl ester oil molecule. The different colors represent the different systems: pure DDAO (blue and yellow), DDAO/ $C_4$  ethyl ester oil (red and gray), and DDAO/ $C_8$  ethyl ester oil (green and cyan).

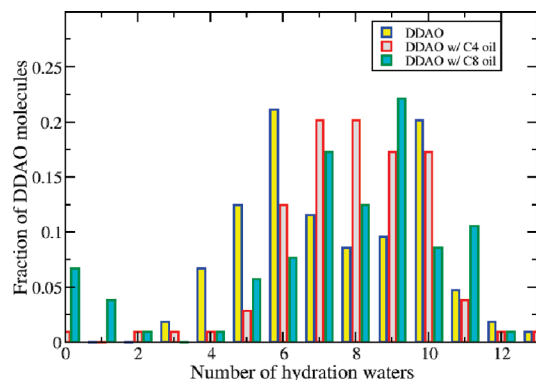


**Figure 9.** Number of hydration water molecules per DDAO molecule. The different colors represent the different systems: pure DDAO (blue and yellow), DDAO/C<sub>4</sub> ethyl ester oil (red and gray), and DDAO/C<sub>8</sub> ethyl ester oil (green and cyan).

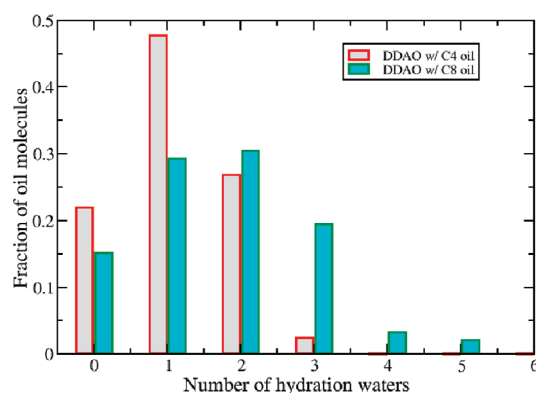


**Figure 10.** Number of hydration water molecules per ethyl ester oil molecule. The different colors represent the different systems: DDAO/C<sub>4</sub> ethyl ester oil (red and gray) and DDAO/C<sub>8</sub> ethyl ester oil (green and cyan).

The total number of hydration water molecules per DDAO molecule in the systems with ethyl ester oil molecules present were calculated using  $n_{\text{hydrateDDAO}} + n_{\text{hydrateoil}} \times N_{\text{oil}}/N_{\text{DDAO}}$ , where  $n_{\text{hydrateDDAO}}$  and  $n_{\text{hydrateoil}}$  are the average number of hydration water molecules per DDAO and ethyl ester oil, respectively, and  $N_{\text{DDAO}}$  and  $N_{\text{oil}}$  are the numbers of DDAO and ethyl ester oil molecules, respectively. From this calculation, the total numbers of hydration water molecules per DDAO are as follows: 7.5 (pure DDAO), 10.3 (DDAO/C<sub>4</sub> ethyl ester oil), and 9.6 (DDAO/C<sub>8</sub> ethyl ester oil). Therefore, as the area per DDAO molecule increases from the pure DDAO system to the DDAO/C<sub>8</sub> ethyl ester oil system to the DDAO/C<sub>4</sub> ethyl ester oil system, the number of hydration water molecules per DDAO also increases.

**3.3. Effect of the Initial Configuration on Pure DDAO Micelles.** The self-assembly of the pure DDAO micelle was also simulated starting from an initial configuration in which the DDAO molecules were placed onto a cubic grid. The self-assembly process was simulated at an elevated temperature of 400 K, and even at that temperature, it took approximately 61 ns before the DDAO molecules had self-assembled into a single micelle. The system was then allowed to equilibrate at a temperature of 300 K for approximately 13 ns. Figure 11 shows a series of snapshots of the DDAO molecules during the course of that simulation. These snapshots show the general process of the micellar self-assembly: the DDAO molecules first form several smaller micelles, and then, these micelles merge either through single chain transfer from one micelle to another or the two

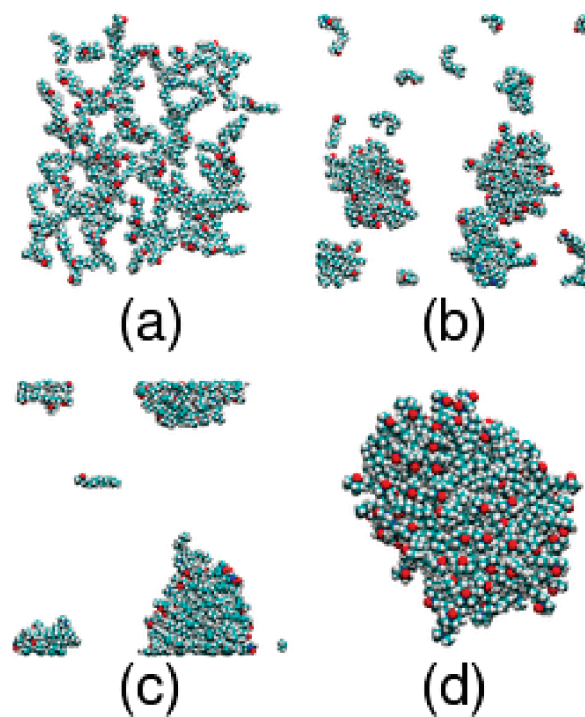


**Figure 11.** Snapshots of the self-assembly process of the DDAO micelle: (a)  $t = 20$  ps, the DDAO molecules are still more or less at their starting points; (b)  $t = 2$  ns, a few smaller micelles have formed but there are still a significant number of lone DDAO molecules in solution; (c)  $t \approx 50$  ns, one large micelle has formed and another smaller micelle still exists and a lone DDAO molecule is being transferred from the small micelle to the large micelle; and (d)  $t \approx 61$  ns the final micelle after the self-assembly process is completed. Note that the water has been removed from the snapshots so that the DDAO molecules can be seen. The same color scheme is used here as in Figure 1.

micelles merging into one larger micelle, until finally one single micelle is formed.

Figure 12a,b displays the number of micelles and the average size of the micelles as a function of time, which provide a quantitative analysis of the self-assembly process of the DDAO micelle. In Figure 12b, the average size of the micelles (red line) is plotted as a function of time, as well as the size of each individual micelle at a given time (black dots). In this analysis, two DDAO molecules are considered to be in a “micelle” if the minimum distance between any two atoms in the molecules is 2.5 Å. Then, a clustering algorithm was used to identify which molecules were in which micelle. For the sake of counting the number of micelles, only the groupings of two or more DDAO molecules were counted; therefore, the lone molecules that do exist particularly during the early stages of the self-assembly process are not represented in the number of micelles in the system.

Initially, this system forms a large number of small micelles which then start to coalesce into fewer large micelles quite rapidly. Within the first 20 ns of the simulation, the system has evolved such that there are 5 micelles: 2 large micelles that are made up of approximately 30 DDAO molecules, 1 micelle with approximately 20 constituent molecules, and 2 smaller micelles. Until 30 ns, the system generally stays in the same state, then one of the large micelles and the medium-sized micelle combine to form one very large micelle that contains more than half of the DDAO molecules. In addition to this very large micelle, two other micelles coexist, made up of approximately 25 and 10 DDAO molecules, respectively. Then after approximately 50 ns, the two larger



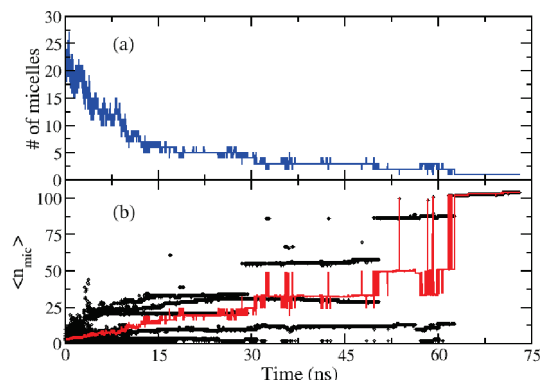


**Figure 12.** (a) Number of micelles as a function of time during the self-assembly process of DDAO molecules that were initially placed on a grid. (b) Size of the micelles within the system as a function of time. The red line shows the average size and the black circles show the size of each individual micelle at a given time in the self-assembly process.

micelles combine to form a micelle which is made up of approximately 87 DDAO molecules, and the smaller micelle remains. Finally after approximately 61 ns, the last two micelles combine to form a micelle which contains all but 1 or 2 lone DDAO molecules, which finally join with the large micelle after about 70 ns.

Similar measurements of the size, shape, and area per chain of the micelle formed during this self-assembly process as in section 3.1 were conducted. In general, very similar results were found for the two systems as summarized in Table 2. In addition, the interfacial properties of the self-assembled micelle are very similar to those for the preassembled micelle (data not shown). Overall, it appears that the preassembled initial configuration results in the same general micelle structure as the more computationally expensive self-assembled micelle.

#### 4. Conclusion

Atomistic molecular dynamics simulations were used to study the structural and interfacial properties of nonionic DDAO micelles with an aggregation number of 104 in pure water. The results of these simulations showed that the micelle is generally ellipsoidal in shape with axial ratios of  $\sim 1.3$ – $1.4$ . The resulting micelle was found to have an area per DDAO molecule of  $94.8 \text{ \AA}^2$ . The average number of hydration water molecules per DDAO molecule was measured to be  $\sim 8$ , and, on average, two water molecules were found to hydrogen-bond to one DDAO molecule. These measures of the shape, area per DDAO molecule, and

**Table 2. Comparison of the Physical Properties of the Pure DDAO Micelle Generated from the Pre-Assembled Starting Configuration and the Pure DDAO Micelle That Resulted from the Self-Assembly of DDAO Molecules<sup>a</sup>**

property	units	preassembled DDAO	self-assembled DDAO
$R_s$	$\text{\AA}$	22.7	22.7
$R_h$	$\text{\AA}$	21.5	21.5
$I_1/I_3$		1.52	1.45
$I_2/I_3$		1.40	1.30
$I_1/I_2$		1.07	1.11
Area/DDAO	$\text{\AA}^2$	94.8	94.8

<sup>a</sup>The properties listed in this table include the micelle radius  $R_s$ , the hydrocarbon core radius  $R_h$ , the three ratios of the moments of inertia ( $I_1/I_3$ ,  $I_2/I_3$ ,  $I_1/I_2$ ), and the area per DDAO molecule of the micelle.

average number of hydration water molecules agree well with the values found experimentally from SANS measurements.<sup>30</sup>

The effect that the presence of  $C_4$  ( $\text{CH}_3(\text{CH}_2)_2\text{COOCH}_2\text{CH}_3$ ) and  $C_8$  ( $\text{CH}_3(\text{CH}_2)_6\text{COOCH}_2\text{CH}_3$ ) ethyl ester oil molecules have on the structural and interfacial properties of the nonionic DDAO microemulsion was also investigated. The microemulsion in the presence of the  $C_4$  oil molecules is less ellipsoidal and more spherical than in the pure DDAO micelle, and the microemulsion in the presence of the  $C_8$  oil molecules is almost a perfect sphere. The  $C_4$  oil molecules were found to move into the core of the micelle, while the  $C_8$  oil molecules remain intermixed with the DDAO molecules in the micelle. Barlow et al.<sup>30</sup> observed the opposite trend when investigating the behavior of medium-chain ( $C_8$ ) and large-chain ( $C_{16}$ ) ethyl ester oils. They found that  $C_8$  ethyl ester oil molecules formed less of a core within the microemulsion than  $C_{16}$  ethyl ester oil molecules. This observation may suggest that maximal core formation occurs with oils that have chain lengths comparable to that of the surfactant molecules in the microemulsion. We plan to conduct more simulations to investigate this further.

Finally, the structural properties of the equilibrated micelle formed from one system starting with DDAO molecules in a “preassembled” spherical micelle and one system starting from DDAO molecules in water were compared. The system that started from individual DDAO molecules in water took  $\sim 61$  ns in order for the molecules to form a micelle. However, all of the DDAO molecules did end up in the final micelle, and the properties of the micelle were nearly identical to those found from the equilibration of the “preassembled” spherical micelle.

**Acknowledgment.** CL acknowledges the KCL Division of Engineering Start-Up funds for supporting this project.